AFRL-RX-WP-JA-2017-0118

CONSTITUTIVE MODEL CALIBRATION VIA AUTONOMOUS MULTIAXIAL EXPERIMENTATION (POSTPRINT)

P.L. Phillips and R. John

AFRL/RX

R.A. Brockman and D.J. Buchanan

University of Dayton Research Institute

11 February 2016
Interim Report

Distribution Statement A.
Approved for public release: distribution unlimited.

© 2017 THE SOCIETY FOR EXPERIMENTAL MECHANICS, INC.

(STINFO COPY)

AIR FORCE RESEARCH LABORATORY
MATERIALS AND MANUFACTURING DIRECTORATE
WRIGHT-PATTERSON AIR FORCE BASE, OH 45433-7750
AIR FORCE MATERIEL COMMAND
UNITED STATES AIR FORCE

REPORT DOCUMENTATION PAGE

Form Approved
OMB No. 0704-0188

The public reporting burden for this collection of information is estimated to average 1 hour per response, including the time for reviewing instructions, searching existing data sources, gathering and maintaining the data needed, and completing and reviewing the collection of information. Send comments regarding this burden estimate or any other aspect of this collection of information, including suggestions for reducing this burden, to Department of Defense, Washington Headquarters Services, Directorate for Information Operations and Reports (0704-0188), 1215 Jefferson Davis Highway, Suite 1204, Arlington, VA 22202-4302. Respondents should be aware that notwithstanding any other provision of law, no person shall be subject to any penalty for failing to comply with a collection of information if it does not display a currently valid OMB control number. **PLEASE DO NOT RETURN YOUR FORM TO THE ABOVE ADDRESS**.

1. REPORT DATE *(DD-MM-YY)*	2. REPORT TYPE	3. DATES COVERED *(From - To)*
2 February 2016	Interim	19 March 2014 – 11 January 2016

4. TITLE AND SUBTITLE
CONSTITUTIVE MODEL CALIBRATION VIA AUTONOMOUS MULTIAXIAL EXPERIMENTATION (POSTPRINT)

5a. CONTRACT NUMBER
IN-HOUSE

5b. GRANT NUMBER

5c. PROGRAM ELEMENT NUMBER

6. AUTHOR(S)
1) P.L. Phillips and R. John - AFRL/RX
2) R.A. Brockman and D.J. Buchanan - UDRI

5d. PROJECT NUMBER

5e. TASK NUMBER

5f. WORK UNIT NUMBER
X0W6

7. PERFORMING ORGANIZATION NAME(S) AND ADDRESS(ES)
1) AFRL/RX
Wright-Patterson AFB, OH 45433
2) University of Dayton Research Institute (UDRI), 300 College Park, Dayton, OH 45409-0110

8. PERFORMING ORGANIZATION REPORT NUMBER

9. SPONSORING/MONITORING AGENCY NAME(S) AND ADDRESS(ES)
Air Force Research Laboratory
Materials and Manufacturing Directorate
Wright-Patterson Air Force Base, OH 45433-7750
Air Force Materiel Command
United States Air Force

10. SPONSORING/MONITORING AGENCY ACRONYM(S)
AFRL/RXCM

11. SPONSORING/MONITORING AGENCY REPORT NUMBER(S)
AFRL-RX-WP-JA-2017-0118

12. DISTRIBUTION/AVAILABILITY STATEMENT
Distribution Statement A. Approved for public release: distribution unlimited.

13. SUPPLEMENTARY NOTES
PA Case Number: 88ABW-2016-0587; Clearance Date: 11 Feb 2016. This document contains color. Journal article published in Conference Proceedings of the Society for Experimental and Applied Mechanics, Vol. 4, 17 September 2016. © 2016 The Society for Experimental Mechanics, Inc. The U.S. Government is joint author of the work and has the right to use, modify, reproduce, release, perform, display, or disclose the work.
The final publication is available at DOI: 10.1007/978-3-319-42028-8_10

14. ABSTRACT *(Maximum 200 words)*
Modern plasticity models contain numerous parameters that can be difficult and time consuming to fit using current methods. Additional experiments are seldom conducted to validate the model for experimental conditions outside those used in the fitting procedure. To increase the accuracy and validity of these advanced constitutive models, software and testing methodology have been developed to seamlessly integrate experimentation, parameter identification, and model validation in real-time over a range of multiaxial stress conditions, using an axial/torsional test machine. Experimental data is reduced and finite element simulations are conducted in parallel with the test based on experimental strain conditions. Optimization methods reconcile the experiment and simulation through changes to the plasticity model parameters. Excursions into less-traveled portions of the multiaxial stress space can be predicted, and then executed experimentally, to identify deficiencies in the model. Most notably, the software can autonomously redirect the experiment to increase the robustness of the plasticity model.

15. SUBJECT TERMS
Axial/torsional experimentation • Plasticity • Constitutive model fitting • Autonomous testing • FEMU

16. SECURITY CLASSIFICATION OF:			17. LIMITATION OF ABSTRACT:	18. NUMBER OF PAGES	19a. NAME OF RESPONSIBLE PERSON (Monitor)
a. REPORT	b. ABSTRACT	c. THIS PAGE			Bill Song
Unclassified	Unclassified	Unclassified	SAR	11	19b. TELEPHONE NUMBER *(Include Area Code)* (937) 255-1351

Chapter 10
Constitutive Model Calibration via Autonomous Multiaxial Experimentation

P.L. Phillips, R.A. Brockman, D.J. Buchanan, and R. John

Abstract Modern plasticity models contain numerous parameters that can be difficult and time consuming to fit using current methods. Additional experiments are seldom conducted to validate the model for experimental conditions outside those used in the fitting procedure. To increase the accuracy and validity of these advanced constitutive models, software and testing methodology have been developed to seamlessly integrate experimentation, parameter identification, and model validation in real-time over a range of multiaxial stress conditions, using an axial/torsional test machine. Experimental data is reduced and finite element simulations are conducted in parallel with the test based on experimental strain conditions. Optimization methods reconcile the experiment and simulation through changes to the plasticity model parameters. Excursions into less-traveled portions of the multiaxial stress space can be predicted, and then executed experimentally, to identify deficiencies in the model. Most notably, the software can autonomously redirect the experiment to increase the robustness of the plasticity model where further deficiencies are identified, thus providing closed loop control of the experiment. This novel process yields a calibrated plasticity model upon test completion that has been fit and more importantly validated, and can be used directly in finite element simulations of more complex geometries.

Keywords Axial/torsional experimentation • Plasticity • Constitutive model fitting • Autonomous testing • FEMU

This paper is declared a work of the U.S. Government and is not subject to copyright protection in the United States.

10.1 Introduction

Due to the high cost of designing and manufacturing complex subcomponents, it is becoming common for finite element analysis to replace experimental tests to avoid the costs associated with elaborate test fixtures and equipment or expensive physical specimens. In addition, certain stress states commonly of interest are difficult, if not impossible, to physically reproduce in experiments. Accurate material models that are calibrated over a wide range of stress and temperature conditions are critical to ensuring the accuracy and reliability of finite element results for complicated geometries subjected to realistic loading environments. Identifying parameters for modern constitutive models, that continue to grow in complexity, is a difficult and time consuming process that has historically be a separate process from the experimental testing. As such, additional experiments are seldom conducted to validate the model for experimental conditions outside those used in the fitting procedure.

Current methods for parameter identification are either separate endeavors as is the case with Finite Element Model Updating (FEMU) [1, 2] or are still limited in the scope of nonlinear models or stress states as is the case with the growing area of the Virtual Fields Method (VFM) [3]. Multiaxial experimentation [4–6], specifically axial/torsional testing [7], is a mature technology and modern equipment is capable of testing at various rates and elevated temperatures; however, material testing is still dominated by tension testing. Finite element methods continue to advance and the constitutive models (including modern plasticity models) used within continue to evolve and grow in complexity as researchers seek to describe

P.L. Phillips (✉) • R.A. Brockman • D.J. Buchanan
University of Dayton Research Institute, 300 College Park, Dayton, OH 45409-0110, USA

Air Force Research Laboratory (AFRL/RXCM), Wright-Patterson AFB, OH 45433-7817, USA
e-mail: Peter.Phillips@udri.udayton.edu

R. John
Air Force Research Laboratory (AFRL/RXCM), Wright-Patterson AFB, OH 45433-7817, USA

© The Society for Experimental Mechanics, Inc. 2017

Y. Zhu, A.T. Zehnder (eds.), *Experimental and Applied Mechanics, Volume 4*,
Conference Proceedings of the Society for Experimental Mechanics Series, DOI 10.1007/978-3-319-42028-8_10

Distribution A. Approved for public release (PA): distribution unlimited.

more complicated behavior, e.g. low-cycle fatigue, non-proportional loading, etc. For an extensive review of modern plasticity models, see Chaboche [8]. Computer hardware has reached the point where multiple CPU systems are relatively inexpensive and parallel processing architectures are readily available in OpenMP and MPI. The maturity of the aforementioned fields enables the advancement of the state-of-the-art in experimental testing through the combination of multiaxial experiments with real-time constitutive model calibration. Software and testing methodology have been developed to seamlessly integrate experimentation, parameter identification, and model validation in real-time over a range of multiaxial stress conditions, using an axial/torsional test machine. The methodology is material agnostic; however, initial work has been focused on initially isotropic materials using phenomenological plasticity models. Upon test completion, this new, novel methodology yields a calibrated plasticity model that has been fit and more importantly validated, and can be used immediately in finite element simulations of more complex geometries. The new method also reduces the time required to perform the complex fitting and decreases the required number and complexity of the test specimens. It also significantly reduces the time to develop a validated model since the experiments are done as needed to fit the model and in real-time as opposed to post-test.

10.2 Methodology

Many different pieces of software are required to perform constitutive model calibration through autonomous multiaxial testing. Figure 10.1 provides an overview of the entire methodology and illustrates how the different pieces of software communicate with each other. Experimental data is reduced and finite element simulations are conducted in parallel with the test based on experimental strain conditions. Optimization methods reconcile the experiment and simulation through changes to the plasticity parameters. Excursions into less-traveled portions of the multiaxial stress space are predicted by the testing platform, and then executed experimentally, to identify deficiencies in the model. Most notably, the software can autonomously redirect the experiment to increase the robustness of the plasticity model where further deficiencies are identified, thus providing closed loop control of the experiment.

The model fitting relies on Finite Element Model Updating (FEMU) which requires both a finite element code and an optimizer. Developing autonomous experimental control of the axial/torsional testing hardware requires software for test control, acquisition of data, and communication with the external software responsible for the overall integration. Section 10.2.1 describes the axial/torsional testing machine and test specimen details. Section 10.2.2 describes the

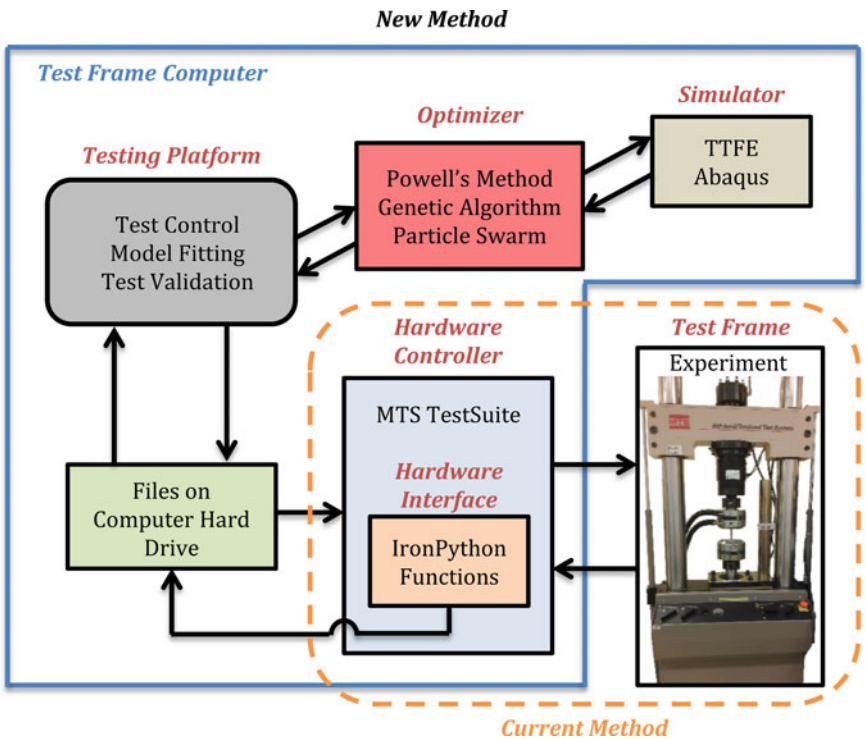

Fig. 10.1 Overview of the new software and test methodology that allows for autonomous multiaxial experimentation and constitutive model fitting

Distribution A. Approved for public release (PA): distribution unlimited.

specialized finite element code written for its compact size, fast execution, and integration with the optimization program. Section 10.2.3 describes the optimization program and the different methods available. Lastly, Sect. 10.2.4 outlines the new novel software responsible for the autonomous constitutive model calibration via multiaxial experimentation.

10.2.1 Experimental Setup

The experiments were conducted on a MTS 809 Axial/Torsional test frame with force and torque capabilities of 100 kN and 1100 N m, respectively. The test frame was controlled using a custom program written in MTS TestSuite. Axial and shear strain measurements were obtained using a MTS high-temperature axial/torsional extensometer with a gage length of 25.0 mm. The specimen used for the initial capability demonstrations was made from 4340 steel, with dimensions as shown in Fig. 10.2.

10.2.2 Simulator (Finite Element Program)

A finite element program has been written that is customized for isotropic materials subjected to axial/torsional loading. This allows for accurate simulation of multiaxial loading for both solid and thin-walled cylindrical specimens made of materials with continuum level isotropic behavior. The code uses axisymmetric, four node elements formulated in cylindrical coordinates with displacement degrees of freedom in the radial, circumferential, and axial directions. Figure 10.3 shows the simplification from the solid three-dimensional mesh to the axisymmetric mesh used in the code. All three degrees of freedom are assumed to be independent of the angular position; therefore, the four node elements are modeled in the theta equals zero plane. The program handles material nonlinearity and implements the material routines through Abaqus/Standard [9] user material subroutines (UMAT) that are written in Fortran. The same material subroutines used in the custom finite element code are directly compatible with the commercial code, Abaqus. Material models for elastic and linear isotropic hardening are also included.

A UMAT has been written for a unified plasticity model with combined nonlinear isotropic-kinematic hardening. The development of the rate equations and the consistent material tangent matrix follows Kirchner [10] with the exception that the yield function has been simplified to include the von Mises stress. This Chaboche type plasticity model has been used successfully by others [8] for the simulation of cyclic experiments. The rate equations describing the model are

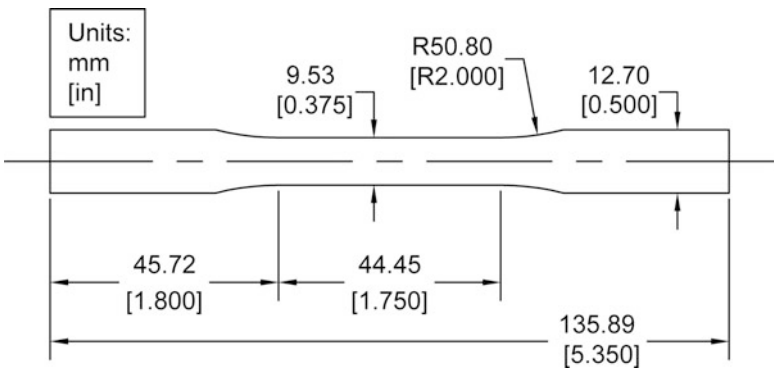

Fig. 10.2 Solid cylindrical specimen made from 4340 steel

Distribution A. Approved for public release (PA): distribution unlimited.

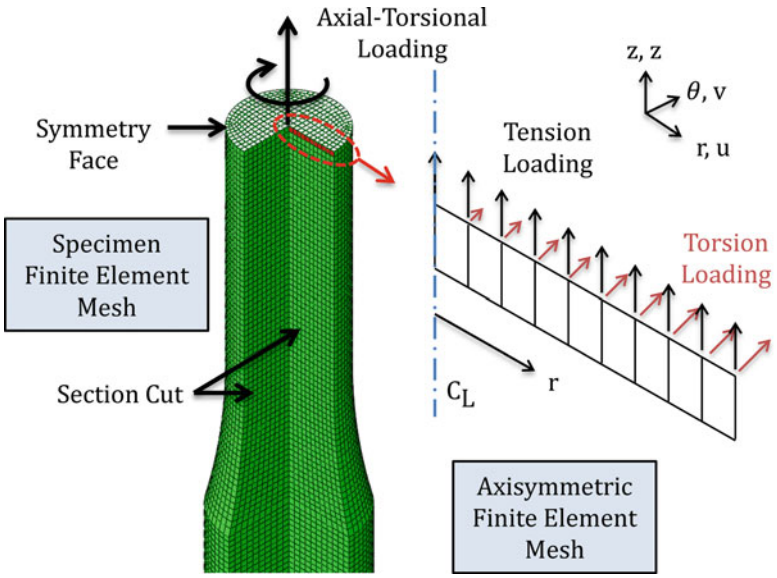

Fig. 10.3 Simplification of a solid cylindrical specimen from three-dimensional solid elements to the axisymmetric elements in polar coordinates used in the custom finite element software

$$
\begin{aligned}
f &= \sqrt{\frac{3}{2}\left(S_{ij}-X_{ij}\right)\left(S_{ij}-X_{ij}\right)} - \rho_0 - \sum_{w=1}^{N}\rho^{(w)} \\
\dot{\sigma}_{ij} &= D_{ijkl}\left(\dot{\varepsilon}_{kl} - \left\langle\frac{f}{D}\right\rangle^{n}\frac{\partial f}{\partial \sigma_{kl}}\right) \\
\dot{\rho}^{(w)} &= b^{(w)}\left(Q^{(w)}-\rho^{(w)}\right)\left\langle\frac{f}{D}\right\rangle^{n} \\
\dot{\chi}_{ij}^{(w)} &= \left(\frac{2}{3}A^{(w)}\frac{\partial f}{\partial \sigma_{ij}} - B^{(w)}\chi_{ij}^{(w)}\right)\left\langle\frac{f}{D}\right\rangle^{n} \\
X_{ij} &= \sum_{w}\chi_{ij}^{(w)} - {}^{1}\!/_{3}\,\delta_{ij}\chi_{kk}^{(w)}
\end{aligned}
\tag{10.1}
$$

where f is the yield function, ρ_0 is the initial yield surface size, $\rho^{(w)}$ are the individual isotropic hardening terms, D is the drag stress, n is the rate sensitivity exponent, and $\chi_{ij}^{(w)}$ are the individual backstress terms. The yield function uses the deviatoric stresses, S_{ij}, and backstresses, X_{ij}. The backstresses have both a linear hardening term, A, and a recovery term, B. The isotropic hardening terms have a saturation stress, Q, and a rate term, b. In addition a series of terms can be used for both the isotropic and kinematic terms to achieve better calibration over multiple strain ranges.

10.2.3 Optimizer

A critical part of the methodology developed is the optimization software as this directly influences to success of the constitutive model fitting. When using FEMU, each objective function evaluation requires a separate call to the finite element program with a different set of material parameters. The optimization seeks to minimize the objective function given in Eq. (10.2), where N is the number of load steps (experimental data points) used in the FE solution, and k denotes the individual load step. The first and second terms of the objective function are related to the force, F, and torque, T, respectively. The subscript 'exp' denotes experimental results while 'FE' denotes finite element results. Each term has a weight factor that can reconcile the difference in magnitude between the force and torque. For this work, w_F is A^{-2} where A is the initial cross-section area, and w_T is r^2J^{-2} where r is the outer radius of the specimen and J is the polar moment of inertia. With the chosen weight factors, the objective function has units of stress squared. The experimental values come directly from the load cell, while the FE values are obtained through integration of element stresses.

Distribution A. Approved for public release (PA): distribution unlimited.

$$obj = \sum_{k=1}^{N} w_F \left(F_{\exp}^{(k)} - F_{FE}^{(k)} \right)^2 + w_T \left(T_{\exp}^{(k)} - T_{FE}^{(k)} \right)^2 \tag{10.2}$$

The optimization software currently has three methods available: Powell's method, a genetic algorithm (GA), and particle swarm optimization (PSO). The three methods have shown to yield fairly similar results when similar inputs and tolerances are used; therefore, the GA and PSO are used as the objective functions can be evaluated in parallel.

The GA is a simple version with concepts taken from Goldberg [11]. The GA uses bound constraints, tournament selection with three parents, uniform crossover, and mutation. Ten parents are used, the probability of crossover and mutation is 0.5 and 0.02, and ten rounds are carried out for a total of 100 objective function evaluations. The PSO has inertia, cognitive, and social factors similar to Kennedy [12] with an additional pheromone velocity factor similar to Foo et al. [13]. The parameter values are bounded through a simple rebound formula in which a particle that exceeds the bounds is reflected at the boundary and the reflected portion loses half its magnitude. Ten particles are used for ten rounds with velocity factors ramped linearly from starting values to end values over the specified number of rounds. Initial and final value pairs for the inertia, cognitive, social factors, and pheromone factors are (0.5, 0.5), (1.0, 2.0), (2.0, 1.0), and (1.0, 1.0) respectively. The initial populations for both methods have been formulated using a Latin-hypercube sampling method similar to Singh et al. [14]. Initial velocities for the PSO are equated to the difference between a second Latin-hypercube population on the initial population. Lastly, velocity clamping is used for the PSO to limit the maximum Euclidean norm of the velocity to 0.33.

10.2.4 Testing Platform

The testing platform software includes the optimizer, simulator, methods to communicate with the MTS test frame through the hardware controller, and additional intelligent algorithms to perform the autonomous multiaxial experimentation and constitutive model fitting. Experimental control is determined on-the-fly rather than requiring the entire process to be predefined because the testing platform software runs simultaneously with the experiment, collects the experimental data, processes the data, and dictates the next loading step for the experiment. The loading steps can be a single ramp from one load level to another, a series of cycles between prescribed load levels, or dwelling at current loads. Control algorithms are included in the testing platform to perform: initial modulus checks for signal verification, zero-load offsets for strain channels based on least-squares regression, yield surface probing for multiple stress trajectories using single specimens (similar to Lissenden et al. [15]), and most importantly, autonomous constitutive model fitting and multiaxial experimentation.

The software can accommodate control modes for load, stroke, and strain implemented through stroke (pseudo-strain). The load and stroke control utilize the built-in capabilities of the test frame controller. However; the pseudo-strain control requires an understanding of the relationship between increments in stroke and corresponding strain increment. This correlation is determined during the initial modulus check. In addition, calculations are done to map the desired strain level to a required stroke, and limit detection is used to stop the load excursion once the requested strain level is reached. As plasticity occurs, the stroke limit predictions based on correlation from elastic deformation will be excessive; however, the strain limit detection stops the stroke at the desired strain. The pseudo-strain method is implemented to bypass the possible instabilities of strain control, and to also allow for the possibility of redundant strain control mechanism (if the extensometer fails or jumps, strain gage data could be used as the controlling signal).

Prior to use in the optimization software, the experimental data is filtered using a lowpass filter. Both eighth-order Butterworth and 100-pole finite impulse response (FIR) filters are available within the software with various cutoff frequencies. The default used is the 100-pole FIR filter with a 10 Hz cutoff. Each loading segment of the filtered data is then further down sampled based on the elastic modulus and user-defined increments in strain over the nonlinear region. This reduces the number of load increments required for the finite element analysis.

The software needs to be initialized with information regarding the desired material model and definitions of the testing boundaries with respect to the axial and shear stress or strain space. Each constitutive model has its own setup routine where the user can prescribe which parameters of the model they wish to optimize. In addition, they can set bounds on the parameter values or accept the default values present in the software. The testing bounds are described in terms of the maximum and minimum levels, or maximum levels and R-ratios where R is the maximum over the minimum load/strain. A sequence of rounds can be prescribed in which the maximum levels increase over each round. Figure 10.4 shows an example for a pseudo-strain-controlled test in which the maximum strain limits were 1.0 % strain. This example also

Distribution A. Approved for public release (PA): distribution unlimited.

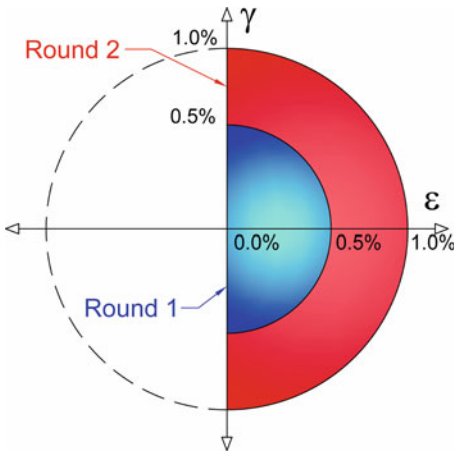

Fig. 10.4 Test conditions for autonomous model fitting with: strain control, ±90° with no compressive strain, and two rounds with a maximum strain of 0.5 and 1.0 %

corresponds to the results presented in the next section. Two rounds are chosen, with the test bounds between ±90° with no compressive strain allowed. The behavior within each round can be predefined by the user or randomly assigned by the software, and each round can consist of multiple stress trajectories within the defined test bounds.

The autonomous fitting procedure directs the experimental test based on the setting for the current round. Force, torque, and strain data from the experiment are read by the software, filtered, and down sampled for use in the optimization program. Some initial portion of the experimental data can be used in the model fitting process, and the remainder can be used for model validation. Plasticity models are history dependent so the entire loading process must be simulated whenever the model parameters are revised. As an example, if the test has a total of three rounds, the first two rounds can be used for the model fitting and the third round can be used for validation to determine the accuracy of the optimized material parameters. The criterion for which data is used in the prediction and which is used for validation is still evolving and will be the focus of future work. In addition, the criteria for when the autonomous fitting procedure has deemed itself converged is continuing to evolve.

10.3 Results

Testing was carried out on a solid cylindrical specimen (Fig. 10.2) made from 4340 steel. Force and torque measurements were obtained from the 100 kN, 1100 N m load and torque cells. Both axial and shear strain data were collected using the axial/torsional extensometer. Prior to starting the fitting procedure, the axial and shear moduli were determined as well as parameters required for using the pseudo-strain algorithm. Rather than perform the yield surface probing, a yield stress of 100 MPa was assumed (based on yield surface probing of a separate specimen). The autonomous model fitting procedure was performed under pseudo-strain control for two rounds with maximum strain levels of 0.5 and 1.0 % strain. Figure 10.4 depicts the test conditions. At each strain level, the specimen underwent: axial only loading (tension only), fully reversed torsional loading, and combined axial and torsional load (again tension only). Figure 10.5 shows experimental results for engineering stress vs. engineering strain for both axial and shear stresses. Both rounds of strain levels were used for the prediction of the material properties. Development of more advanced algorithms for the model fitting and validation data set definitions will continue to evolve as more experience is gained in working with the new software.

The plasticity model with nonlinear isotropic and kinematic hardening given in Eq. (10.1) was used during the modeling fitting procedure. A single isotropic hardening term was used (with two parameters b and Q), and two nonlinear kinematic hardening terms were used. The first kinematic term used both parameters A1, and B1, while the second kinematic term only used the linear parameter A2, with the corresponding recovery parameter B2 set to zero. The optimization was therefore performed for a total of five material parameters (b, Q, A1, B1, and A2). Both the GA and PSO were used for comparison of the methods with settings as described in the *Optimizer* section.

Table 10.1 provides results for the optimized material parameters, and also provides computation times for each algorithm. Both algorithms were run using two computer processors (thus two FE jobs are run simultaneously). Preliminary scalability testing of the parallelization has shown a scalability factor of 0.92 out of 1.0. Both optimization methods converged on similar material parameters, and the objective function values are in reasonable agreement. Figure 10.6 compares the stresses from the experiment with the stresses from the best set of parameters resulting from the GA and PSO.

Distribution A. Approved for public release (PA): distribution unlimited.

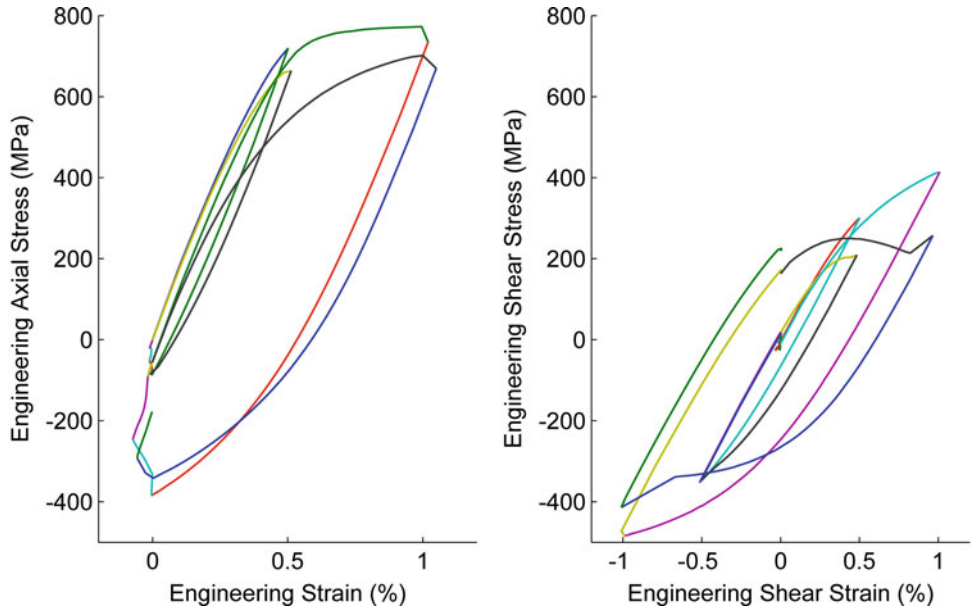

Fig. 10.5 Strain controlled experimental results for solid cylindrical specimen made of 4340

Table 10.1 Material property fitting optimization results for both GA and PSO

Method	Computer cores	Number of analyses	Run time (min)	Run time (s)	Obj fun.
GA	2	100	23.6	1414	4,373,610
PSO	2	100	16.2	969	3,607,640
	Par	**GA**	**PSO**	**min**	**max**
	Q	250	224	10	250
	b	5520	4550	500	9000
	A1	290,370	108,160	50	9,000,000
	A1/B1	297	341	10	1000
	B1	976	317	5	9000
	A2	3,226,500	5,846,300	1000	10,000,000
	B2	–	–		

The optimized set of parameters follow the same trends as the experiment, but there is room for improvement. Changes to the control settings of the optimization methods will likely reduce the difference in peak magnitudes between the experimental and FE results. Work is ongoing to improve the optimization control settings.

10.4 Conclusions

To increase the accuracy and validity of modern plasticity models, software and testing methodology have been developed to seamlessly integrate experimentation, parameter identification, and model validation in real-time over a range of multiaxial stress conditions, using an axial/torsional test machine. This novel process can yield a calibrated plasticity model upon test completion that has been fit and more importantly validated, and can be used directly in finite element simulations of more complex geometries. This work is a significant step in advancing how materials are tested in the laboratory and characterized using constitutive models. The new methods can produce calibrated models in real-time for multiaxial conditions (rather than the predominate trend of uniaxial testing) and will likely require less time and fewer specimens. The methodology is material independent and the finite element software and material models could be extended to anisotropic materials if desired. Future work will focus on improving the fitting and validation algorithms, and applying the new testing methodology to materials of interest in the aerospace community, namely nickel-based superalloys and titanium.

Distribution A. Approved for public release (PA): distribution unlimited.

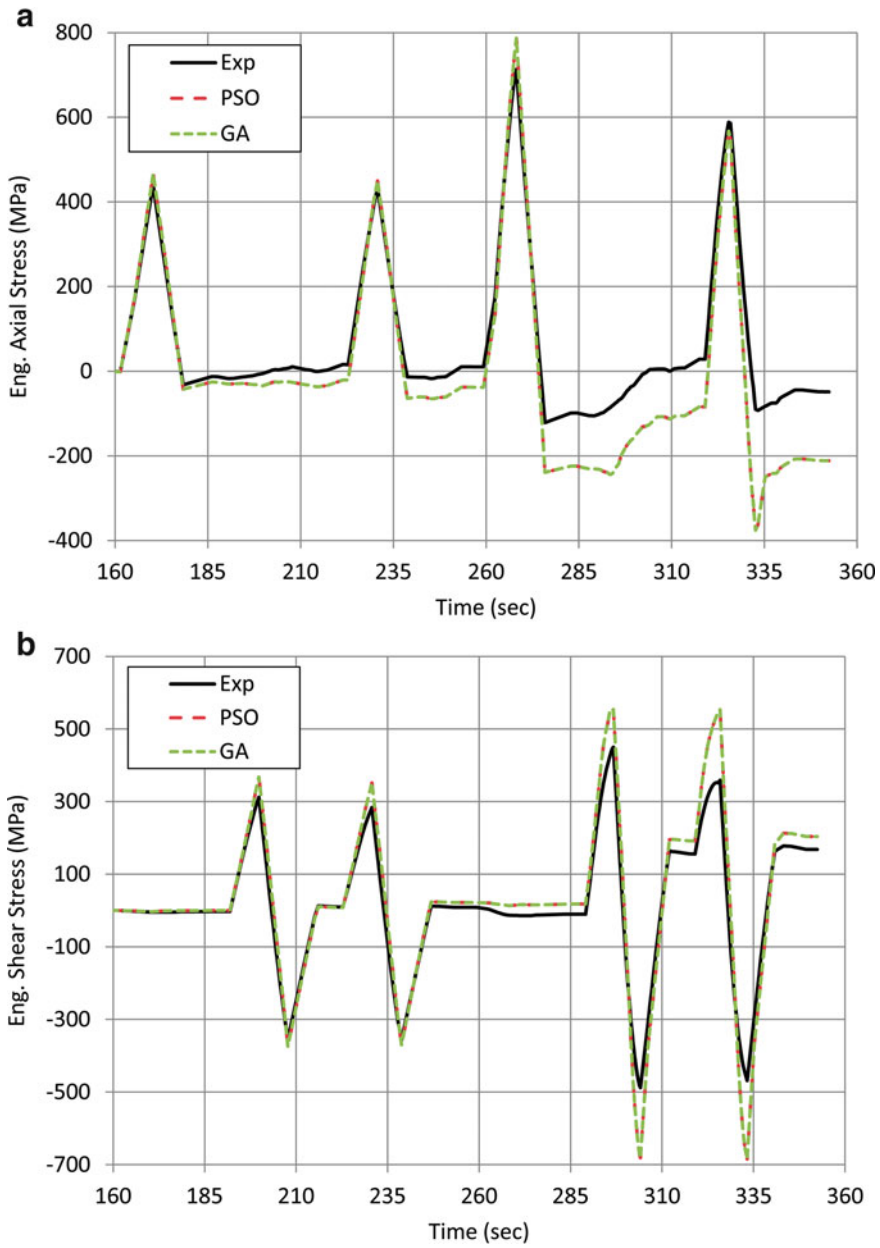

Fig. 10.6 Comparison of the (**a**) axial stress and (**b**) shear stresses from the experiment (*solid line*) and the nearly identical results from the GA and PSO optimization (both *dashed*)

Acknowledgements This work has been sponsored through the AFRL/DAGSI Ohio Student-Faculty Research Fellowship program, Topic RX14-12. Additional funding assistance was also provided through the Air Force Research Laboratory, AFRL/RXCM, Wright-Patterson Air Force Base, OH, under DoD contract FA8650-14-D-5205.

The authors would like to thank the Air Force Research Laboratory, AFRL/RXCM for the use of their axial/torsional testing equipment and Mr. Philip E. Blosser for his assistance in operating the equipment.

References

1. Fedele, R., Filippini, M., Maier, G.: Constitutive model calibration for railway wheel steel through tension–torsion tests. Comput. Struct. **83**(12–13), 1005–1020 (2005)
2. Avril, S., Pierron, F., Sutton, M.A., Yan, J.: Identification of elasto-visco-plastic parameters and characterization of Lüders behavior using digital image correlation and the virtual fields method. Mech. Mater. **40**(9), 729–742 (2008)
3. Pierron, F., Grédiac, M.: The Virtual Fields Method. Springer, New York (2012)
4. Guest, J.J.: On the strength of ductile materials under combined stress. Proc. Phys. Soc. Lond. **17**(1), 202 (1899)

Distribution A. Approved for public release (PA): distribution unlimited.

5. Osakada, K.: History of plasticity and metal forming analysis. J. Mater. Process. Technol. **210**(11), 1436–1454 (2010)
6. Michno Jr., M.J., Findley, W.N.: An historical perspective of yield surface investigations for metals. Int. J. Non Linear Mech. **11**(1), 59–82 (1976)
7. Cailletaud, G., Kaczmarek, H., Policella, H.: Some elements on multiaxial behaviour of 316 L stainless steel at room temperature. Mech. Mater. **3**(4), 333–347 (1984)
8. Chaboche, J.L.: A review of some plasticity and viscoplasticity constitutive theories. Int. J. Plast. **24**(10), 1642–1693 (2008)
9. Dassault Systemes: ABAQUS User's Manual, Version 6.13. Dassault Systemes Inc. (2013)
10. Kirchner, E.: Modeling single crystals: time integration, tangent operators, sensitivity analysis and shape optimization. Int. J. Plast. **17**(7), 907–942 (2001)
11. Goldberg, D.E.: Genetic Algorithms in Search, Optimization, and Machine Learning, 30. Print. Addison-Wesley, Boston (2012)
12. Eberhart, R.C., Kennedy, J.: A new optimizer using particle swarm theory, In: Proceedings of the Sixth International Symposium on Micro Machine and Human Science, vol. 1, pp. 39–43 (1995)
13. Foo, J.L., Kalivarapu, V., Winer, E.: Implementation of digital pheromones for use in particle swarm optimization (2006)
14. Singh, G., Spradlin, T.J., Grandhi, R.V.: Fatigue life optimization using a laser peening process, In Proceedings of the 50th AIAA/ASME/ASCE/AHS/ASC Structures, Structural Dynamics, and Materials Conference, Palm Springs, California (2009)
15. Lissenden, C.J., Lerch, B.A., Ellis, J.R., Robinson, D.N.: Experimental determination of yield and flow surfaces under axial-torsional loading. ASTM Spec. Tech. Publ. **1280**, 92–112 (1997)

Distribution A. Approved for public release (PA): distribution unlimited.